# FRAGILITY AND RELIABILITY ANALYSES OF SOIL - PILE - BRIDGE PIER INTERACTION

## *UDC 624.21:699.841*

# Mladen Ćosić[1], Radomir Folić[2], Boris Folić[3]

[1]Institute for Testing of Materials - IMS, Belgrade, Serbia
[2]University of Novi Sad, Faculty of Technical Sciences, Novi Sad, Serbia
[3]University of Belgrade, Innovative Centre, Faculty of Mechanical Engineering, Belgrade, Serbia

**Abstract**. *The purpose of this paper is to present the methodology for performance-based seismic evaluation of soil-pile-bridge pier interaction using the incremental nonlinear dynamic analysis (INDA). The system's input signal was treated through the generated artificial accelerograms which were subsequently processed by soil layers and for the bedrock. The INDA analysis was post processed separately for the pier and for the pile, so that the constructed PGA=f(DR) curves are in the capacitive domain. For these curves the authors identified the performance levels, while the regression analyses were conducted based on the specific DR and PGA parameters. Fragility curves were constructed based on the solutions of regression analysis and the probability theory of log-normal distribution. Based on the results of fragility analysis, reliability curves were also constructed. The methodological procedure for seismic performance analysis presented in this study provides an integrated quantitative-qualitative consideration and evaluation of the complex soil-foundation-structure interaction (SFSI).*

**Key words**: *incremental nonlinear dynamic analysis, pile performance, fragility, reliability, artificial accelerograms.*

## 1. INTRODUCTION

Due to the complexity of phenomena involved in the wave propagation in soil-structure interaction (SSI), mathematical modelling of this problem is based on a multidisciplinary approach to the engineering seismology and earthquake engineering. The soil-structure interaction can be considered by conducting tests on actual models and/or in the laboratory, using analytical and numerical methods. The development of

modern codes for designing structures has been enhanced by taking into account the earthquake action, the level of security against premature collapse and non-ductile behaviour. However, given the stochastic nature of earthquakes and the complexity of the soil-structure interaction phenomenon, mathematical models and analyses dealing with this problem should be improved continuously. The soil-foundation-structure interaction (SFSI) is considered for both shallow and deep funding such as piles. The contemporary Performance-Based Earthquake Engineering (PBEE) methodology provides a more complete and sophisticated understanding and treatment of the SFSI through hazard analysis, structural analysis, damage analysis and loss analysis [1], [2]. Using the PBEE methodology, the analysis of structural response under seismic actions may be considered in time (TDA - time domain analysis), frequency (FDA - frequency domain analysis) and capacitive (CDA - capacity domain analysis) domains, analyzing the structure's bearing capacity and deformation in a particular case of piles.

The PBEE-based pile performance research methodology and the EQWEAP procedure developed for that purpose is described in [3], while the use of incremental dynamic analysis (IDA) for analyzing groups of piles is discussed in [4] and [5]. Seismic performances are considered in several ways: by applying the deterministic concept with a single earthquake scenario, based on parametric analysis and the probabilistic concept. The paper [6] presents a 3D finite element incremental dynamic analysis study of caisson foundations carrying single-degree of freedom (SDOF) structures on clayey soil. The emphasis is given to the interplay between the nonlinearities developed above (superstructure) and, mainly, below ground surface, either of material (soil plasticity) or of geometric (caisson–soil interface gapping and slippage) origin. The pile performance analysis by establishing a correlation between the engineering demand parameters (EDP) and the intensity measure (IM) is presented in [7]. The general approach of modelling the dynamic interaction of piles groups in the soil using the hybrid techniques by connecting the finite element method (FEM) and the boundary element method (BEM) is discussed in [8], while the various aspects of mathematical and numerical modelling of the complex soil-piles interaction are presented in [9]. General approaches to analyzing the seismic performance of piles with the emphasis on various mathematical soil-pile interaction models are presented in [10], while the interaction effects in evaluations of the system ductility demand ratio (DDR) are discussed in [11]. Modelling the piles and soil using 3D finite elements and taking into account the influence of plastic nonlinear soil behaviour in seismic performance assessment is presented in [12]. Analysis of seismic response of pile groups using the 3D solid FEM for piles and the soil is discussed in [13], while the method of 3D continuum for analyzing the seismic response is presented in [14]. The seismic performance analysis of the pile to pile cap connection is discussed in [15] using the FEM method and the study of this phenomenon was based on the damage to actual connections.

A large body of scientific research which is devoted to modelling the behaviour and analyzing the response of soil-pile systems is considered in the time domain of nonlinear dynamic analysis (NDA) or the capacitive domain of nonlinear static pushover analysis (NSPA). There is a considerably fewer number of soil-pile interaction studies based on the incremental dynamic analysis (IDA). Therefore, the concept of this work is focused on modelling the aspects of soil-pile interaction based on the INDA analysis, the application of which is discussed in the section of numerical simulation where the results are also presented. In order to understand and complete the methodology of these analyses, in

addition to the incremental nonlinear dynamic analysis, the following was also considered: numerical modelling of soil-pile interaction and the generation of artificial accelerograms. Results of numerical simulations were presented and 300 NDA analyses were statistically processed.

## 2. NUMERICAL MODELLING OF THE SOIL-PILE INTERACTION

In creating the mathematical and corresponding numerical soil-pile interaction model there are several phases: concretization, abstraction and discretization. The specific problem is defined in the concretization phase by considering separately the domains of soil, piles and the structure above ground level. Through the phase of abstraction, the actual physical soil-pile model is replaced by specific mathematical and numerical model, respectively, while in the discretization phase the predefined domains are transformed into subdomains. There are several approaches to modelling and analyzing the soil-pile interaction based on the finite element method, taking into account the development of geometric and material nonlinearity; they are the following:
- piles: 1D finite elements; soil: implicitly, based on the elements of interaction,
- piles: 1D finite elements; soil: 2D and 3D finite elements,
- piles: 2D finite elements; soil: implicitly, based on the elements of interaction,
- piles: 2D finite elements; soil: 2D finite elements,
- piles: 3D finite elements; soil: implicitly, based on the elements of interaction,
- piles: 3D finite elements, soil: 3D finite elements.

From the continuous numerical model, the soil-pile interaction system is translated into a discrete numerical model, while the principle of discretization allows modelling the sub domains behaviour at a very high level. The principle of approximation used in this study is based on modelling the pile and structure by liner finite elements, while the soil was modelled implicitly through replacement elements. Figure 1a shows the actual pile model in the soil and with the structure above ground level (bridge pier). Figure 1b shows the numerical pile model formed from linear finite elements, and with the structure above ground level.
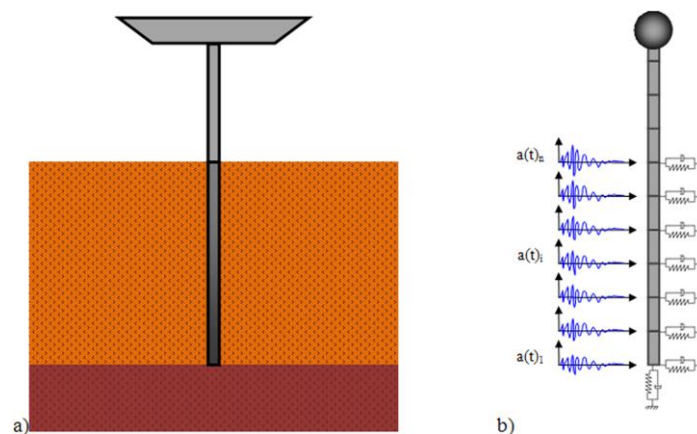


**Fig. 1** a) the realistic model of pile in the soil, bridge pier and soil, b) the numerical model of pile, bridge pier and implicit modelling of soil action

The linear finite elements for modelling the pile and the bridge pier are based on the principle of propagation of nonlinear deformation along the element, where at the cross section level a specific fibre discretization is implemented. The cross-section is generally considered through three sub domains: unconfined concrete, confined concrete and steel. The stress-strain state at the cross section level is determined by integrating the nonlinear single-axis stress-strain state of each single fibre [16]. The above described linear finite elements are implemented into the SeismoStruct software [17]. According to Mander [18], the constitutive model of behaviour for the unconfined and confined domains of concrete is a nonlinear constant confinement concrete model, in which four parameters define mechanical properties. The first parameter $f_{ck}$ is the concrete compressive strength, as defined by a 150x300mm cylindrical sample at age of 28 days according to EC 2 [19]:

$$f_{ck,c} = f_{ck}\left(1 + 5\frac{\sigma_2}{f_{ck}}\right) \qquad \text{for} \quad \sigma_2 \leq 0.05 f_{ck}$$
$$f_{ck,c} = f_{ck}\left(1.125 + 2.5\frac{\sigma_2}{f_{ck}}\right) \quad \text{for} \quad \sigma_2 > 0.05 \text{f}_{ck} \tag{1}$$

where $\sigma_2$ is the effective lateral compressive stress due to confinement, and $\gamma_c$ is the bulk density of concrete. The second parameter is $f_{ctk}$ the strength of concrete under axial tension:

$$f_{ctk} = k_t \sqrt{f_{ck}} , \tag{2}$$

where $k_t$=0.5 for axial tension, and $k_t$=0.75 for bending tension. The third parameter $\varepsilon_{c,max}$ is the concrete strain under maximum compressive stress, while the fourth parameter $k_c$ is the factor related to the ratio between the confined and unconfined compressive stress in concrete.

The constitutive model of behaviour of steel reinforcement is a bi-linear elastic-plastic model with kinematic strain hardening in the nonlinear deformation zone [20], where the following applies for the elastic domain:

$$\sigma_s = E_s(\varepsilon_s - \varepsilon_{s,p}) , \tag{3}$$

where $\sigma_s$ is the stress in steel reinforcement, $E_s$ is the modulus of elasticity of steel reinforcement, $\varepsilon_s$ is the strain of steel reinforcement, $\varepsilon_{s,p}$ is the plastic strain of steel reinforcement. The law of flow rule is defined by:

$$\dot{\varepsilon}_{s,p} = \gamma \text{sign}(\sigma_s - q) , \tag{4}$$

while the law of isotropic and kinematic hardening by:

$$\dot{q} = \gamma H \text{sign}(\sigma_s - q) , \quad \dot{\alpha} = \gamma , \tag{5}$$

where the condition for yielding is:

$$f(\sigma_s, q, \alpha) := |\sigma_s - q| - [\sigma_{s,y} + K\alpha] \leq 0$$
$$E_\sigma = \{(\sigma_s, q, \alpha) \in \Re \times \Re^+ \times \Re \mid f(\sigma_s, q, \alpha) \leq 0\} \tag{6}$$

while the Kuhn-Tucker complementary conditions:

$$\gamma \geq 0, \qquad f(\sigma_s, q, \alpha) \leq 0, \qquad \gamma f(\sigma_s, q, \alpha) = 0, \tag{7}$$

and the condition of consistency:

$$\gamma \dot{f}(\sigma_s, q, \alpha) = 0. \tag{8}$$

Defining the mechanical properties of the constitutive model of steel reinforcement behaviour requires the following three parameters. The first is $E_s$ the modulus of elasticity of steel reinforcement, the second is $\sigma_{s,y}$ the stress at the yield point of reinforcement steel and the third is $\mu_s$ the ratio of post-elastic stiffness $E_{s,p}$ and the initial elastic stiffness $E_s$ (strain hardening parameter), where:

$$E_{s,p} = \frac{\sigma_{s,ult} - \sigma_{s,y}}{\varepsilon_{s,ult} - \dfrac{\sigma_{s,y}}{E_s}}, \tag{9}$$

where $\sigma_{s,ult}$ is the maximum stress value in steel reinforcement and $\varepsilon_{s,ult}$ is the maximum value of strain of steel reinforcement, while $\gamma_s$ is the specific weight of steel reinforcement.

The finite element type by which the pile and pier are modelled is the inelastic displacement-based frame element [21]. This type of finite element has six degrees of freedom $\theta_{A,y}$, $\theta_{A,z}$, $\theta_{B,y}$, $\theta_{B,z}$, $\Delta_a$, $\theta_T$, with the corresponding internal forces and moments $M_{A,y}$, $M_{A,z}$, $M_{B,y}$, $M_{B,z}$, $N$, $M_T$. Geometric nonlinearity is introduced by applying the effects of large displacement and rotation and through the P-Δ effects. The equilibrium and compatibility conditions are established on the deformed configuration using the co-rotational formulation [22].

The nonlinear dynamic soil-pile interaction (SPI) is modelled using the constitutive model of behaviour for the lateral analysis of piles, where the formation of gaps under cyclic soil deformation is also taken into account [23]. Effects of cyclic degradation/hardening of soil stiffness and strength are also taken into account; in addition, actions in the direction pile axis are also separately modelled, which are orthogonal to the effects that are introduced by applying this model of interaction. The hysteretic constitutive model consists of four major parts: backbone curve, standard reload curve (SRC), general unload curve (GUC) and direct reload curve (DRC). The backbone curve is an adaptive polygonal curve defined by four segments [24]:

$$p(y) = \sum_{i=1}^{j} (p_i - p_{i-1}) + \alpha_j K_0 (y - y_j), \quad j = \max(i), \ \forall y_i \leq y, \ j \geq 0, \tag{10}$$

where: $p$ is the soil response, $y$ is the relative displacement, $\alpha_j$ is the stiffness reduction coefficient in the last curve segment and $K_0$ is the initial stiffness. Defining the mechanical properties of the constitutive model of the soil-pile interaction behaviour requires nineteen parameters: $K_0$ initial stiffness, $F_c$ soil strength ratio at the first turning point $0 \leq F_c < 1$, $F_y$ yielding soil strength, $P_0$ initial force ratio at zero displacement $0 \leq P_0 \leq 0.9$, $P_a$ minimum force ratio at baseline $0 \leq P_a \leq P_0$, $P_a \leq \beta_n F_y$ and $P_a \leq F_c$, $\alpha$ stiffness ratio after first turning point $0.001 \leq \alpha \leq 1$, $\alpha_n$ unloading stiffness factor, $\beta$ yielding stiffness ratio, $\beta_n$ ultimate soil strength ratio $\beta_n < 1$ for $\beta < 0$, $\beta_n = 1$ for $\beta = 0$, $\beta_n > 0$ for $\beta > 0$, $Flg$ flag settings combination indicator adjustment factor 1 out of 31 combinations in defining the constitutive model, $e_{p1}$ is DRC starting stiffness ratio, $p_1$ gap force parameter $0 \leq p_1 \leq 1$, $p_2$ soil cave-in parameter, $p_k$ and $e_k$ are stiffness degradation/hardening parameters, $p_s$ and $e_s$ are strength degradation/hardening

parameters, $k_s$ slope of the S-N curve and $f_0$ soil stress corresponding to point $S_1$ in S-N curve. The hysteretic damping ratio $\xi_h$ of the model ranges from 0, for a perfectly elastic response, to the largest possible amount of energy dissipation per cycle under two-way cyclic loading [24]:

$$\xi_h = \begin{cases} \dfrac{1}{2\pi}\left[2 - \dfrac{K_s}{K_0}\right] \\ \dfrac{1}{2\pi}\left[2 - \dfrac{K_s}{K_0} - \left(\dfrac{K_s}{K_0}\right)\left(1 - \dfrac{1+\phi}{\phi/\phi_1}\right)^2\left(\dfrac{1}{\alpha_1} - 1\right)\right] \end{cases} \text{ for } \begin{array}{l} \phi \le \dfrac{\phi_1}{1-\phi_1} \\ \phi > \dfrac{\phi_1}{1-\phi_1} \end{array} , \tag{11}$$

where $\varphi_i = p_i/p_f$, and $K_s$ is the secant stiffness.

## 3. GENERATION OF ARTIFICIAL ACCELEROGRAMS

Generation is a procedure of creating artificial accelerograms based on defined procedures in the frequency domain [25]. This is a highly favourable procedure of creating accelerograms, considering that a ground motion record (GMR) can be created for the designed range of responses determined either by the deterministic or probabilistic concept. Also, this accelerogram is scaled and matched to the given response spectrum.

The procedure of generating artificial accelerograms is conducted by determining the spectral density function based on the response spectrum; in this specific case a pseudo response spectra has been used [26]. This function is used to derive the sinusoidal signal amplitude the phase angle of which is generated by a random number function in the range between $0 \div 2\pi$ according to uniform distribution. Sinusoidal signals are compressed in order to generate accelerograms. In order to determine the other properties of the artificial accelerogram, such as duration of recording, it is necessary to obtain additional information about the expected earthquake based on the response spectrum. Any periodic function can be developed into a sine wave [27]:

$$x(t) = A_0 + \sum_i A_i \sin(\omega_i t + \phi_i) , \tag{12}$$

where $A_i$ is the amplitude, and $\varphi_i$ is the phase angle. The amplitude $A_i$ is correlated with the function of spectral density $G(\omega)$:

$$A_i = \sqrt{2\int_0^{\omega_i} G(\omega_i)d\omega} , \tag{13}$$

while the relation between the response spectrum and the function of ground motion spectral density is given through:

$$G(\omega_n) = \dfrac{1}{\omega_n\left[\dfrac{\pi}{4\xi_s} - 1\right]}\left\{\left(\dfrac{\omega_n S_v}{r_{s,p}}\right)^2 - \int_0^{\omega_n} G(\omega)d\omega\right\}^{1/2} , \tag{14}$$

where:

$$\xi_s = \frac{\xi}{1 - e^{-2\xi\omega_n t}} \; , \; r_{s,p} = [2\log\{2n(1 - e^{-\delta_y(s)\sqrt{\pi\log 2n}})\}]^{1/2} \; , \; \delta_y(s) = \left(\frac{4\xi t}{\pi}\right)^{1/2} \; , \; n = \frac{-\omega_n t}{2\pi\log 0.368} \; , \quad (15)$$

where $S_v$ is spectral velocity and $\xi$ is the damping coefficient. The accelerogram generated by the above described procedure still fails to present the amplitude of the actual accelerogram model. To this end, it is necessary to define the acceleration envelope for the preliminary generated accelerogram:

$$X(t) = a(t) = I(t)\sum_i A_i \sin(\omega_i t + \phi_i) \; . \quad (16)$$

In addition to the stationary envelope, trapezoidal and exponential envelopes have also been used, as well as a model of complex envelope where both the initial and final domains, and in particular the domain of strong motion, are separately defined.

Upon the generation of artificial accelerograms for representing the record of the free field motion, further analyses are conducted in order to generate accelerograms for soil layers and bedrock motion. In this specific case, the soil is considered as a single-layer system, but given the number of input accelerograms in numerical analyses for simultaneous performance of numerical integration in time, the single-layer system is considered as a multi-layer system with the same geo-technical properties. For each individual layer accelerograms are generated taking that waves are propagating similar to the single-layer system. Generally, the mathematical formulation of the transverse wave propagation in a single-layer system $s$ and the bedrock $r$ is as follows [28]:

$$u_s(z_s,t) = A_s e^{i(\omega t + k_s^* z_s)} + B_s e^{i(\omega t - k_s^* z_s)} \; , \qquad u_r(z_r,t) = A_r e^{i(\omega t + k_r^* z_r)} + B_r e^{i(\omega t - k_r^* z_r)} \; , \quad (17)$$

where $\omega$ is the angular frequency and $k^*$ is the complex wave number. By resolving equation (17), the following is obtained:

$$A_r = \frac{1}{2} A_s \left[(1 + \alpha_z^*)e^{ik_s^* H} + (1 - \alpha_z^*)e^{-ik_s^* H}\right] , \; B_r = \frac{1}{2} A_s \left[(1 - \alpha_z^*)e^{ik_s^* H} + (1 + \alpha_z^*)e^{-ik_s^* H}\right] , (18)$$

$$A_s = \frac{2A}{(1 + \alpha_z^*)e^{ik_s^* H} + (1 - \alpha_z^*)e^{-ik_s^* H}} \; . \quad (19)$$

The accelerogram for bedrock is generated by applying the transfer function $F(\omega)$, which is the ratio between the amplitudes for the terrain surface and the bedrock:

$$F(\omega) = \frac{1}{\cos k_s^* H + i\alpha_z^* \sin k_s^* H} \; . \quad (20)$$

## 4. INCREMENTAL NONLINEAR DYNAMIC ANALYSIS

The soil-pile interaction responses are considered in the capacity analysis domain using a series of nonlinear dynamic analysis (NDA), or incremental nonlinear dynamic analysis (INDA). Accelerograms are scaled successively from the initial minimum scaling

factor $F_{s,0}$ through the ultimate scaling factor $F_{s,n}$ for state of collapse. First, it is the scaling to a specific initial value, so that the structure's response to a given scaled level of earthquake is in the linear-elastic domain. This is achieved by scaling the accelerogram to a sufficiently low value of acceleration [29]:

$$PGA_{s,1} = F_{s,1} PGA_{us}, \qquad (21)$$

where $PGA_{us}$ is the maximum acceleration of original un-scaled accelerogram, $F_{s,1}$ is the start scaling factor for the NDA analysis, and $PGA_{s,1}$ is the maximum acceleration of the scaled accelerogram scaled to the initial minimum acceleration value. The scaling is continued by increasing $PGA_{s,i}$ in a successive manner:

$$PGA_{s,i} = PGA_{s,i-1} + 0.1 + 0.05(i-1) \qquad \text{for} \quad i = 1,...n, \qquad (22)$$

and when it is observed that the difference in the structure's response for two consecutive scaling values is without any major changes, then the scaling factor is increased. In the case when the difference in the structure's response to the two subsequent scaling values is significant, then the scale factor is reduced. If the NDA analysis for the $PGA_{s,i}$, shows that the maximum drift value is:

$$DR_{\max} \rightarrow + \propto, \qquad (23)$$

then the scaling is done according to:

$$PGA_{s,i+1} = PGA_{s,i-1} + \frac{(PGA_{s,i} - PGA_{s,i-1})}{3}, \qquad (24)$$

while the following applies to the scale factors:

$$F_{s,1} < F_{s,i} < F_{s,n}. \qquad (25)$$

The required number of nonlinear dynamic analyses (NDA) within a single incremental nonlinear dynamic analysis (INDA) is defined by [30]. Figure 2 shows the pushover INDA curve *IM=f(EDP)* constructed based on the interpolation of discrete values $I_i(EDP_i, IM_i)$ from the NDA analyses for scaling accelerograms from the elastic, through non-linear and up to the collapse domain. Values of the engineering demand parameter EDP and the intensity measure IM are given on the abscissa and the ordinate, respectively.
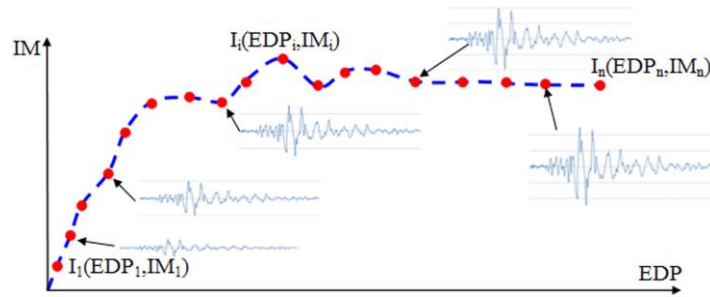


**Fig. 2** The INDA pushover curve *IM=f(EDP)* with discrete values
from the NDA analyses and scaled accelerograms [25]

The INDA analysis used in this study is equivalent to the term of the existing IDA (incremental dynamic analysis) analysis INDA≡IDA, provided if the IDA analysis is a complete nonlinear analysis with the development of both geometric and material nonlinearities in the system. In the procedure of determining the acceleration, velocity and displacement of the soil-pile interaction, in terms of earthquake actions, the differential equations of motion are the following:

$$[M]\{a\} + [C]\{v\} + [K]\{d\} = \{Q\} . \tag{26}$$

Solving equation (26) is carried out by a step by step numerical integration using the Hilber-Hughes-Taylor (HHT) method in its modified form [31]:

$$[M]\{a\}_{i+1} + (1+\alpha)[C]\{v\}_{i+1} - \alpha[C]\{v\}_i + (1+\alpha)[K]\{d\}_{i+1} - \alpha[K]\{d\}_i = \{Q\}_{i+\alpha} , \tag{27}$$

and for a given moment of time:

$$t_{i+1} = t_i + \Delta t , \tag{28}$$

where $[M]$ is the mass matrix, $\{a\}$ is the acceleration vector, $[C]$ is the damping matrix, $\{v\}$ is the velocity vector, $[K]$ is the stiffness matrix, $\{d\}$ is displacement vector and $\{Q\}$ is the vector of externally generated forces. Displacement and velocity vectors are expressed by:

$$\{d\}_{i+1} = \{d\}_i + \Delta t\{v\}_i + \frac{\Delta t^2}{2}[(1-2\beta)\{a\}_i + 2\beta\{a\}_{i+1}] , \tag{29}$$

$$\{v\}_{i+1} = \{v\}_i + \Delta t[(1-\gamma)\{a\}_i + \gamma\{a\}_{i+1}], \tag{30}$$

while for the vector of externally generated forces the following applies:

$$\{Q\}_{i+\alpha} = \{Q\}(t_{i+\alpha}), \tag{31}$$

where:

$$t_{i+\alpha} = (1+\alpha)t_{i+1} - \alpha t_i = t_{i+1} + \alpha\Delta t . \tag{32}$$

The HHT method becomes unconditionally stable if parameters $\alpha$, $\beta$ and $\gamma$ are selected according to the following relations:

$$\alpha \in \left[-\frac{1}{3}, 0\right], \quad \beta = \frac{1}{4}(1-\alpha)^2, \quad \gamma = \frac{1}{2} - \alpha . \tag{33}$$

Correction of the system's stiffness matrix is carried out after each step, and it is based on the Newton-Raphson's incremental-iterative method.

## 5. NUMERICAL SIMULATION RESULTS AND DISCUSSION

Numerical simulations of nonlinear pile behaviour in interaction with the soil were carried out using the finite element method in the SeismoStruct software [17]. In the pre-processing stage, the numerical parameters of the model were defined separately for each domain according to the previously presented mathematical formulation. The pile and pier diameter is $d_p$=1.8m, the pile length is $L_p$=15m, while the bridge pier height is $L_b$=10m. The pier and pile are of circular cross-section with radially disposed reinforcement consisting of 25 rods of Ø40mm diameter. The cross-section is discretized to 300 fibres, and a total of 10 integration

sectors were considered. The mass applied to the pier top is $m=816$t. The constitutive concrete model is defined for the C 25/30 strength class, according to EC 2 [19]: $f_{ck}=25$MPa, $f_{ctk}=0$, $\varepsilon_{c,max}=2.1^0/_{00}$ and $\gamma_c=24$kN/m³ for the unconfined and confined concrete domain, $k_c=1$ for the unconfined concrete domain and $k_c=1.2$ for the confined concrete domain. The real value of the concrete strength under the pressure of $f_{ck,calc}=30$MPa for the confined concrete domain is higher than the nominal value of $f_{ck}=25$MPa, since it is multiplied with $k_c$. For the purposes of this research the effects of tensile stress in the concrete were annulled $f_{ctk}=0$, while the global coefficient $k_c$ is used as the ratio of unconfined and confined compressive stress in concrete. The constitutive model of steel reinforcement is also defined according to EC 2 [19]: $E_s=200$GPa, $f_{s,y}=435$MPa, $\mu_s=0.01$ and $\gamma_s=78.5$KN/m³. The following are the parameters of the constitutive model of soil-pile interaction: $K_o=15000$KN/m³, $P_0=0$, $P_a=0$, $\alpha=0.5$, $\alpha_n=1$, $\beta=0$, $\beta_n=1$, $Flg=31$, $e_{p1}=1$, $p_1=1$, $p_2=0$, $p_k=1$, $e_k=1$, $p_s=1$, $e_s=1$ and $k_s=0.1$. Parameters $F_c$ and $F_y$ are determined in the function of changes along the soil depth, so that these values were separately identified for the 16 link elements used for modelling the soil-pile interaction based on the $p$-$y$ curves. Thus, at the soil depth of $h=1$m: $F_c=0.338$ and $F_y=118.2$KNm, while on the soil depth of $h=5$m: $F_c=0.645$ and $F_y=1298.2$KNm.

The artificial accelerograms were generated using the Simqke software [32] for the horizontal elastic response spectra according to EC 8 [33] for type C soil, where the shear wave velocity $v_{s,30}=290$m/s, the peak ground acceleration $PGA=0.35$g, the soil coefficient $S=1.2$, damping ratio $\xi=5\%$, and the number of cycles of improving the fitting of the response spectra of the generated accelerograms $n_f=100$. The $n_f$ value greatly influences the generation of artificial accelerograms, as its increase severely influences the frequency content of accelerograms [25]. On the other hand the increase of this value results in a somewhat higher number of local acceleration peaks which values tend to the absolute value of peak acceleration. Two groups were considered, each with five artificial accelerograms. The first group consists of accelerograms of shorter total time of acceleration recording $t_{acc}=20$s and a shorter time of stationary domain, where the times of stationary domain initiation and finalization are $t_{s,i}=2$s and $t_{s,f}=10$s, respectively (Figure 3a). The second group consists of accelerograms with longer total time of acceleration recording $t_{acc}=40$s and a longer time of stationary domain, where the times of stationary domain initiation and finalization are $t_{s,i}=2$s and $t_{s,f}=15$s, respectively (Figure 3b). Accelerograms were sampled at a time interval of $\varDelta t=0.01$s, so that sampling frequency is $f_s=100$Hz. For all generated artificial accelerograms, $PGA$ is obtained to be $0.437$g.
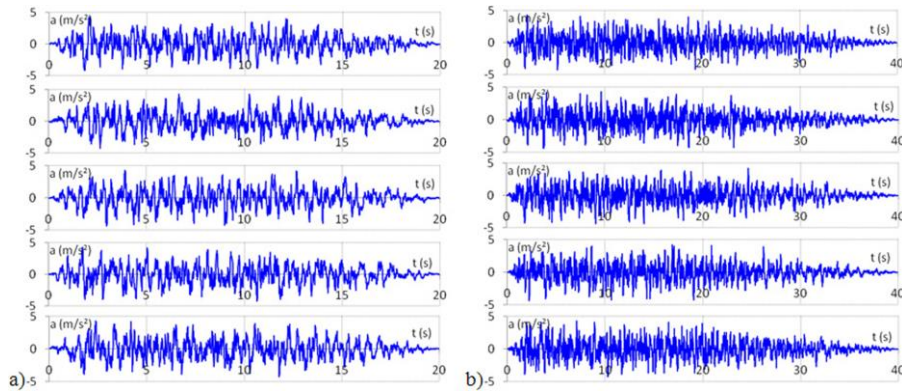


**Fig. 3** The generated artificial accelerograms for:
a) $t_{s,i}=2$s, $t_{s,f}=10$s, $t_{acc}=20$s, b) $t_{s,i}=2$s, $t_{s,f}=15$s, $t_{acc}=40$s

After the accelerograms were generated, they were further processed in the Shake software [34], in order to generate independent accelerograms along the soil depth $a(t)_i$ (Figure 4). The soil domain is discretized to 15 soil layers of 1m thickness, while the bedrock domain is considered separately, so that for each INDA analysis 16 simultaneous accelerograms were used in the processing phase. A total of 160 accelerograms were generated in this manner. In INDA analyses, these accelerograms were simultaneously scaled, so that for a single INDA analysis all 16 accelerograms were scaled with the same scale factor. First, accelerograms were scaled to the initial value of $PGA_{s,1}$=0.1g for $h$=0 and then incrementally scaled to $\Delta PGA$=0.1g. Given the differences among the accelerograms and the scale factors according to Figure 4, the ultimate scale factors among the accelerograms for a single INDA analysis are also different. Due to the large number of generated accelerograms, they are not presented in this paper; instead, only the values of *PGA* changes along the soil depth were provided. For each INDA analysis, accelerograms were scaled to *PGA*=3g, so the total of 300 NDA analysis were carried out. By processing the INDA analyses the discrete values $I_i(EDP_i,IM_i)$ were obtained, which were then interpolated and represent the system response in the capacitive domain. For the EDP parameter, a global drift (*DR*), while for the IM parameter a *PGA* was selected. Figures 5 and 6 are depicting the *DR-PGA* ratio curves for the pier top and the pile head, respectively.
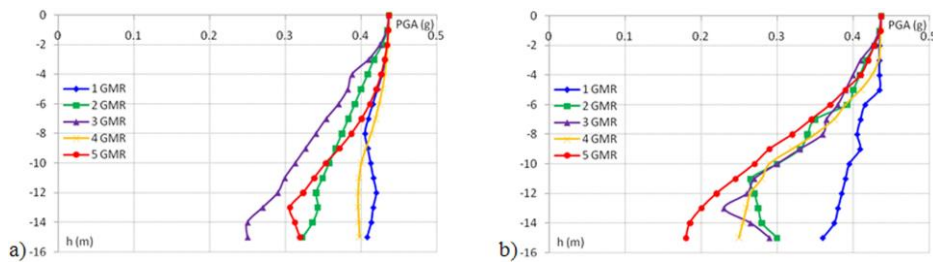


**Fig. 4** Changes of the *PGA* along the soil depth for the generated artificial accelerograms:
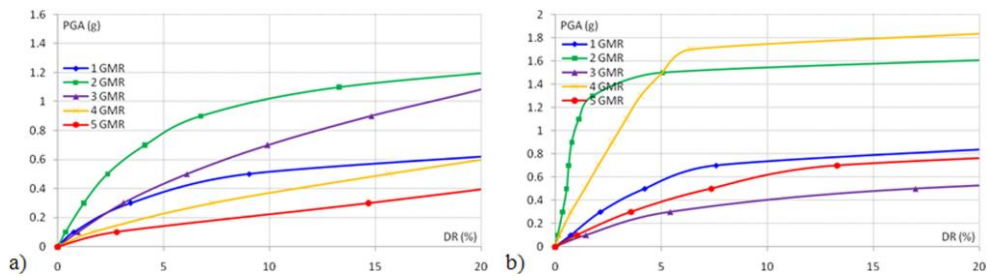a) the first group, b) the second group



**Fig. 5** The *DR-PGA* curve for the pier top: a) the first group of accelerograms, b) the second group of accelerograms
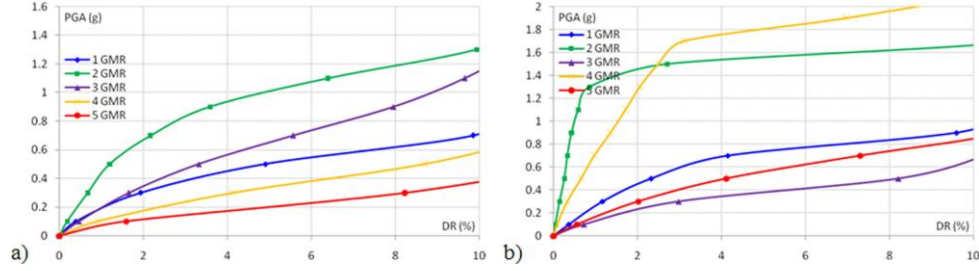
**Fig. 6** The *DR-PGA* curve for the pile head: a) the first group of accelerograms,
b) the second group of accelerograms

Generally, it can be concluded that there is a discrepancy in the soil-pile system response for two different groups of accelerograms, first with $t_{acc}$=20s and second with $t_{acc}$=40s total acceleration recording time. A difference also exists when considering the pier and pile response, where slightly higher *PGA* values were registered for the pile, as compared to the pier. The drift interval value for the pier is considered in the range of *DR*=[0÷20]%, while for the pile this range was *DR*=[0÷10]%. The limit states of the soil-pile system were determined by considering the structural performance level (SPL): immediate occupancy (IO), collapse prevention (CP) and the global dynamic instability (GI). The issue of determining the limit states of the system can be resolved via the EDP or IM parameters, by calculating the corresponding parameter IM for the given EDP. For the purpose of the present study, the appropriate limit state for the IM parameter has been established based on the EDP parameter according to codes. The IO performance level is determined by considering the *PGA* value for the global drift $DR_{IO}$ of reinforced concrete systems according to SEAOC [35] and FEMA 356 [36]:

$$0.5\% \leq DR_{IO} \leq 1\%, \ PGA_{IO} = DR_{IO} \cap (PGA = f(DR)), \ DR_{IO} = \frac{D_{IO}}{H}, \qquad (34)$$

where $D_{IO}$ is the displacement for the IO performance level and *H* is the height. The CP performance level is determined when the tangent slope to the *PGA=f(DR)* curve is equal to 20% of the initial elastic slope $DR_e$ of this curve or when *DR*=10%:

$$DR_{CP} = \min\begin{cases} 20\%DR_e \\ 10\% \end{cases}, \quad PGA_{CP} = DR_{CP} \cap (PGA = f(DR)), \quad DR_{CP} = \frac{D_{CP}}{H}, \ (35)$$

where $D_{CP}$ is the displacement for CP performance level. The GI performance level is determined for the condition that the *PGA=f(DR)* curve asymptotically approaches the horizontal line:

$$DR_{GI}, PGA_{GI} : \frac{PGA_i - PGA_{i-1}}{DR_i - DR_{i-1}} \to 0, \ PGA_{GI} = DR_{GI} \cap (PGA = f(DR)), \ DR_{GI} = \frac{D_{GI}}{H}, \ (36)$$

where $D_{GI}$ is the displacement for the GI performance level. Based on the above set criteria for determining the performance level, statistical analyzes were conducted for each *PGA=f(DR)* curve. Results of these analyzes are shown in Table 1, sorted separately

for the pier and pile. Tags in the table are as follows: $PGA_m$ mean value of the maximum acceleration values, $PGA_{med}$ median value of the peak acceleration values, $PGA_{min}$ minimum value of peak accelerations, $\sigma$ standard deviation, $v$ variance. Discrete values of specific $PGA_i$ performance levels for the soil-pile interaction, separately with respects of the pier and pile, respectively, are shown in Figures 7 and 8. The number of discrete values (samples) is shown on the abscissa, while the $PGA_i$ values, as determined according to the previously described methods, are shown on the ordinate.

**Table 1** Discrete $DR_i$ and $PGA_i$ values of specific performance levels
for the soil-pile interaction

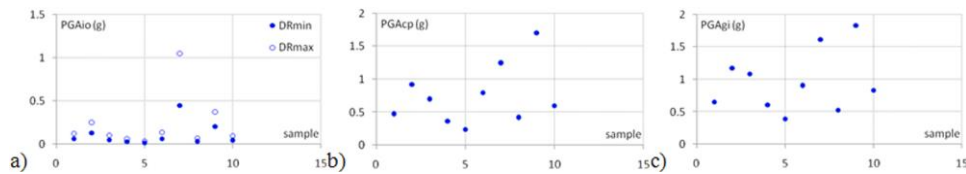| performance level | | IO$_{min}$ | | IO$_{max}$ | | CP | | GI | |
|---|---|---|---|---|---|---|---|---|---|
| | | | | | pier | | | | |
| $DR_m$ (%) | $PGA$ (g) | 0.5 | 0.11 | 1 | 0.23 | 8.32 | 0.75 | - | 0.96 |
| $DR_{med}$ (%) | $PGA$ (g) | 0.5 | 0.06 | 1 | 0.11 | 10 | 0.65 | - | 0.87 |
| $DR_{min}$ (%) | $PGA$ (g) | 0.5 | 0.02 | 1 | 0.04 | 1.4 | 0.24 | 18.6 | 0.39 |
| $\sigma$ | | 0.132 | | 0.305 | | 0.446 | | 0.473 | |
| $v$ | | 0.017 | | 0.093 | | 0.199 | | 0.223 | |
| | | | | | pile | | | | |
| $DR_m$ (%) | $PGA$ (g) | 0.5 | 0.22 | 1 | 0.36 | 6.71 | 0.88 | - | 1.03 |
| $DR_{med}$ (%) | $PGA$ (g) | 0.5 | 0.11 | 1 | 0.20 | 7.35 | 0.80 | - | 0.90 |
| $DR_{min}$ (%) | $PGA$ (g) | 0.5 | 0.03 | 1 | 0.07 | 0.9 | 0.36 | - | 0.36 |
| $\sigma$ | | 0.290 | | 0.387 | | 0.420 | | 0.535 | |
| $v$ | | 0.084 | | 0.150 | | 0.176 | | 0.287 | |



**Fig. 7** Discrete *PGA* values of specific performance levels for the pier: a) IO, b) CP, c) GI
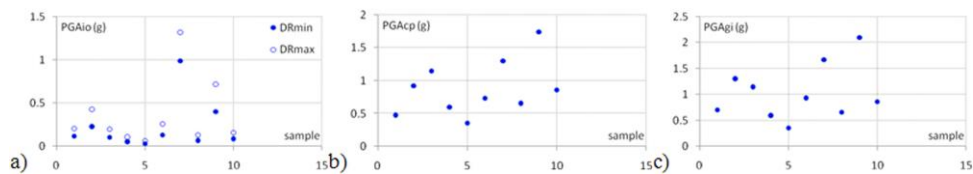


**Fig. 8** Discrete *PGA* values of specific performance levels for the pile: a) IO, b) CP, c) GI

The determination of the $PGA_{IO}$ intensity measure for the IO performance criterion is always a function of fixed value of $DR_{IO}$. However, the $PGA_{CP}$ intensity measure for the CP performance criterion can be oscillating to a significant degree. In this specific case, a lower drift value has been realized of $DR_{min}$=0.9% for the CP performance level, as compared to the drift value of $DR_{min}$=1% for the $IO_{max}$ performance level at the pile head.

The consequence of this situation is that the pile can much faster develop the state of pre-collapse in the second group of accelerograms. The determination of the GI performance level is much more complicated as compared to the previous IO and CP performance levels, since, in certain situations, the $PGA=f(DR)$ curve does not need to approach the horizontal line asymptotically. More precisely, it is obligatory that the $PGA=f(DR)$ curve is horizontal; in many cases, however, this condition is optional, unless the sign of inclination of the $PGA=f(DR)$ curve changes from positive to negative value. This condition is achieved only in one case, in $DR_{min}=18.6\%$ and $PGA=0.39g$ for the pier, while in other cases the GI performance level is determined based on the maximum drift value.

Unlike the previously presented deterministic methods of evaluation of performance levels and the conditions of the soil-pile interaction system, based on the theory of probability it is possible to consider the system's fragility. The probabilistic concept in the analysis of the soil-pile interaction system is based on a qualitative consideration of the damage level according to HAZUS [37]: slight, moderate, extensive and complete. These damage levels are defined as a function of the system ductility $\mu$, so that the level of slight damage is equivalent to $1<\mu<2$, the level of moderate damage is equivalent to $2<\mu<4$, the level of extensive damage is equivalent to $4<\mu<7$, while the level of complete damage is equivalent to $\mu>7$ [38]. The intensity parameter IM is commonly considered by identifying the appropriate response spectra with the variation of standard deviation $\pm\sigma$, which is a function of uncertainty of the seismic demand that is imposed to the structure. However, in this study, a variation of seismic demand is applied which is a function of scaling the IM parameter, i.e. the $PGA$, according the INDA analysis. In this sense, it is possible to consider a much wider range of seismic demand variations $PGA=[0\div1]g$ without any further extrapolation. The relation between $\mu$ and $PGA$ was determined based on regression analysis for the linear function of $\ln\mu=k\cdot\ln PGA+n$, so that the following was obtained for the pier (Figure 9a):

$$\ln\mu = 1.325\cdot\ln PGA + 3.644, \tag{37}$$

while for the pile (Figure 9b):

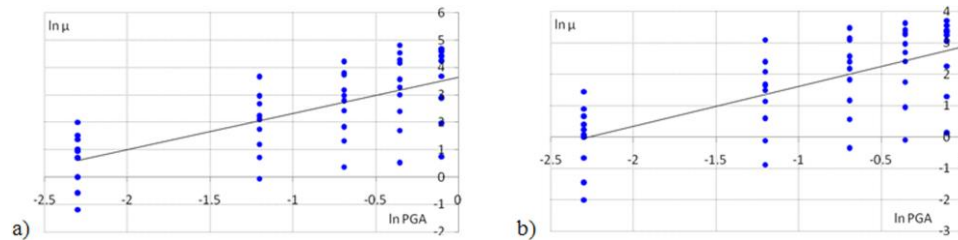$$\ln\mu = 1.272\cdot\ln PGA + 2.877. \tag{38}$$



**Fig. 9** Regression analysis for the *DR* and *PGA* relation: a) pier, b) pile

The fragility curve was constructed in relation to the *PGA* intensity measure by using the log-normal distribution, the probability density function of which is:

$$f(PGA, m, \sigma) = \frac{1}{PGA\,\sigma\sqrt{2\pi}} e^{-\frac{(\ln(PGA)-m)^2}{2\sigma^2}}, \tag{39}$$

where $m$ is the mean $PGA$ value. The cumulative distribution function on the occurrence of damage is determined by [39]:

$$P = F(PGA, m, \sigma) = \frac{1}{2}\mathrm{erfc}\left(-\frac{\ln PGA - m}{\sqrt{2}\sigma}\right) = \Phi\left(\frac{\ln PGA - m}{\sigma}\right), \tag{40}$$

where *erfc* is the complementary error function and $\Phi$ is the cumulative distribution function. The discrete probability functions for the pier and pile are shown in Figures 10a and 10b, respectively. A lower level of damage is typical up to $PGA$=0.2g for the pier model, while for the pile, this value is up to $PGA$=0.3g. The cumulative probability distribution function of damage for the seismic soil-pile interaction is shown in Figures 11a and 11b for the pier and pile, respectively. The upper limit of the complete damage level is considered for $\mu_{sup}$=20, whereby the changes of this limit significantly affect the cumulative probability distribution function of complete damage. By comparing the obtained solutions for the pier and pile, it can be concluded that the pier is more sensitive to the changing levels of intensity measures $PGA$. The consequence of this is that the same $PGA$ level results in larger damage to the pier, where the development higher intensity damage is also more likely. Typical values for seismic intensity measures $PGA$=[0.1÷0.5]g and the corresponding probabilities of fragility $P_i$ for seismic soil-pile interaction are shown in Table 2. Values of fragility probability beneath the diagonal in Table 2 are typically equivalent to 1 or very close to this value, while those above the diagonal are typically equivalent to 0 or very close to this value. The values on the diagonal itself and near to it in Table 2 are declining. If, for example, the value of $PGA$=0.1g, then it can be concluded that at all fragility levels of the pier are higher than that of the pile. Thus, for the level of slight damage, the probability of pier and pile fragility are equal to $P$=0.88 and $P$=0.04, respectively, while for the level of extensive damage this value is $P$=0 for both the pier and the pile. On the other hand, for $PGA$=0.3g, the probability of pier and pile fragility for the level of slight damage are $P$=1, while for the level of extensive damage is $P$=0.99 and $P$=0.03, respectively.
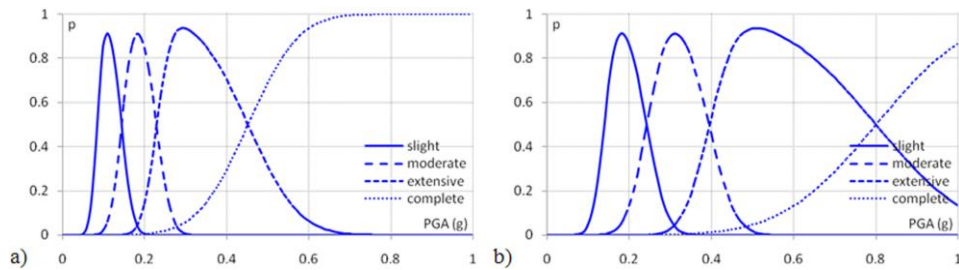


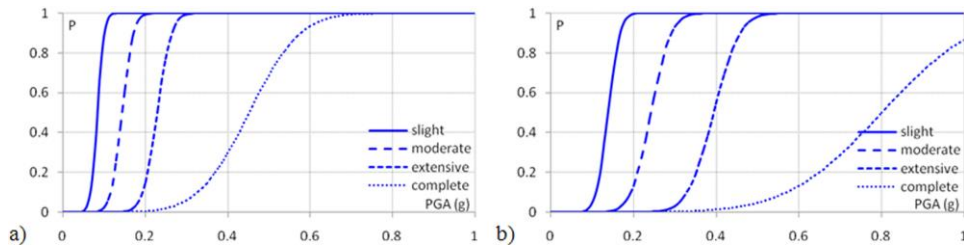**Fig. 10** Discrete probability functions: a) pier, b) pile

**Fig. 11** Fragility curves for seismic soil-pile interaction: a) pier, b) pile

**Table 2** Probability of fragility $P_i$ for the typical seismic
intensity measure $PGA_i$ of the soil-pile interaction

| | | pier | | | pile | | | |
|---|---|---|---|---|---|---|---|---|
| damage | slight | moderate | extensive | complete | slight | moderate | extensive | complete |
| $PGA$=0.1g  $P_i$ | 0.88 | 0.02 | 0 | 0 | 0.04 | 0 | 0 | 0 |
| $PGA$=0.2g  $P_i$ | 1 | 0.99 | 0.15 | 0 | 0.99 | 0.13 | 0 | 0 |
| $PGA$=0.3g  $P_i$ | 1 | 1 | 0.99 | 0.06 | 1 | 0.93 | 0.03 | 0 |
| $PGA$=0.4g  $P_i$ | 1 | 1 | 1 | 0.29 | 1 | 1 | 0.55 | 0.01 |
| $PGA$=0.5g  $P_i$ | 1 | 1 | 1 | 0.69 | 1 | 1 | 0.98 | 0.05 |

Evaluation of the system performance is also performed by analyzing the system reliability state. When applying this analysis a more complete answer is obtained regarding the system state, and it is based on the previously considered fragility analysis. System reliability $R$ is defined by [40]:

$$R = \Phi^{-1}(1-P). \tag{41}$$

A negative $R$ coefficient value indicates a possible failure and system unreliability, while a positive $R$ coefficient value indicates that the failure probability is approximately equal to 0, i.e. that the system is reliable to a significant degree. When the $R$ coefficient value is ≈6, then the system reliability is ≈100%, while in the case when $R$≈0, the system failure probability is $P$=50%. Reliability curves for the seismic soil-pile interaction are shown in Figures 12a and 12b for the pier and pile, respectively. Comparing the solutions obtained for the pier and pile, it can be concluded that the pier is more sensitive to the changing levels of intensity measure $PGA$, so that higher levels of uncertainty can be expected at lower $PGA$ values, as compared to the pile. Typical values of seismic intensity measure of $PGA$=[0.1÷0.5]g and the corresponding values of reliability coefficient $R_i$ for the seismic soil-pile interaction are shown in Table 3. Values of reliability probability beneath the diagonal in Table 3 are typically negative, while those above the diagonal are typically positive. The values on the diagonal itself and near to it in Table 3 are increasing. For $P$>50%, pier reliability at slight level of damage is $PGA$≤0.08g, at moderate level of damage is $PGA$≤0.14g, at extensive level of damage is $PGA$≤0.22g and at complete level of damage is $PGA$≤0.45g. For $P$>50%, pile reliability at slight level of damage is $PGA$≤0.13g, at moderate level of damage is $PGA$≤0.24g, at extensive level of damage is $PGA$≤0.39g and at complete level of damage is $PGA$≤0.8g.
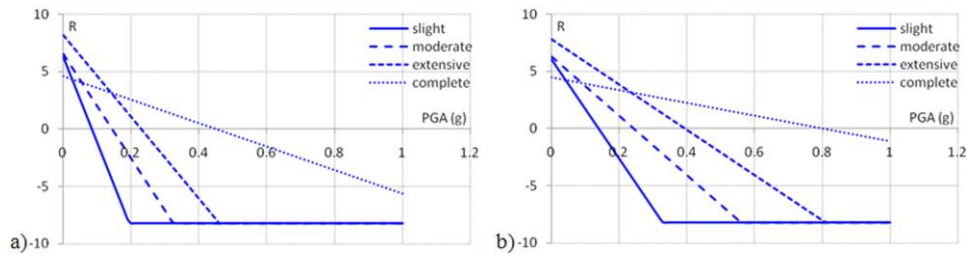
**Fig. 12** Reliability curves for the seismic soil-pile interaction: a) pier, b) pile

**Table 3** Values of reliability coefficient $R_i$ for typical seismic
intensity measures $PGA_i$ of the soil-pile interaction

| | | pier | | | pile | | | |
|---|---|---|---|---|---|---|---|---|
| damage | slight | moderate | extensive | complete | slight | moderate | extensive | complete |
| $PGA$=0.1g  $R_i$ | -1.17 | 2 | 4.60 | 3.61 | 1.70 | 3.71 | 5.85 | 3.90 |
| $PGA$=0.2g  $R_i$ | -8.22 | -2.54 | 1.04 | 2.59 | -2.65 | 1.12 | 3.86 | 3.35 |
| $PGA$=0.3g  $R_i$ | -8.22 | -7.09 | -2.52 | 1.56 | -7.01 | -1.48 | 1.87 | 2.79 |
| $PGA$=0.4g  $R_i$ | -8.22 | -8.22 | -6.08 | 0.54 | -8.22 | -4.07 | -0.12 | 2.23 |
| $PGA$=0.5g  $R_i$ | -8.22 | -8.22 | -8.22 | -0.49 | -8.22 | -6.67 | -2.11 | 1.68 |

## 6. SUMMARY AND CONCLUSIONS

In this study, a numerical model has been developed for the soil-pile-bridge pier interaction in order to evaluate the system's seismic performance. The pier and pile were modelled according the principles of concretization, abstraction and discretization in numerical analysis using the finite element method. Effects representing the influence of soil were introduced by applying the principle of implicit modelling the nonlinear dynamic soil-pile interaction. The input signal to the system is treated through the generated artificial accelerograms, which were further processed by layers of soil and bedrock. The system response is analyzed in the capacitive domain using the incremental nonlinear dynamic analysis (INDA). The INDA analysis was processed in a successive manner by scaling the nonlinear dynamic analysis (NDA) according the defined scaling criteria.

The NDA and INDA analyses were post processed according to the global drift $DR$ and the corresponding $PGA$ values separately for the pier and separately for the pile, so that curves $PGA=f(DR)$ were constructed in the capacitive domain. The IO, CP and GI performance levels were determined for these curves, and based on specific $DR$ and $PGA$ parameters regression analyses were carried for the linear function $\ln\mu=$k·$\ln PGA+n$. The fragility curves were constructed based on the solutions of regression analysis and the probability theory of log-normal distribution for the $PGA$ intensity measures. The intensity parameter $IM$ is typically considered by identifying the corresponding response spectra with the variation of standard deviation $\pm\sigma$, which is a function of uncertainty of seismic demand that is imposed to the structure. However, in this study the authors applied a variation of seismic demand in a function of scaling the $IM$ parameter, or $PGA$ according to the INDA analysis. In this sense, it is possible to consider a much wider range of variation in seismic demand $PGA=[0\div1]$g without any further extrapolation. By

comparing the obtained solutions of the fragility curve for the pier and pile, it can be concluded that the pier is more sensitive to the changing levels of intensity measure *PGA*, than the pile. Thus, the same *PGA* level results in larger damage to the pier, where the development of higher intensity damage is also more likely. Based on the solutions obtained in fragility analysis, reliability curves were also constructed. By comparing the obtained solutions for the pier and pile, it can be concluded that the pier is more sensitive to the changing levels of intensity measure *PGA*, so that it can develop higher levels of uncertainty at lower *PGA* values, as compared to the pile. The methodological procedure for seismic performance analysis presented in this study provides an integrated quantitative and qualitative consideration and evaluation of the complex soil-foundation-structure interaction (SFSI).

REFERENCES

1.  H. Krawinkler, Challenges and progress in performance-based earthquake engineering, International Seminar on Seismic Engineering for Tomorrow - In Honor of Professor Hiroshi Akiyama, Tokyo, Japan, 1999.
2.  J. Moehle, H. Krawinkler, A framework methodology for performance-based earthquake engineering, The 13th World Conference on Earthquake Engineering, Paper No. 679, Vancouver, Canada, 2004.
3.  D. Chang, T. Yang, C. Yang, Seismic performance of piles from PBEE and EQWEAP analyses, Geotechnical Engineering Journal of the SEAGS & AGSSEA, 41(2) (2010) 1-8.
4.  M. Cubrinovski, B. Bradley, Assessment of seismic performance of soil-structure systems, The 18th NZGS Geotechnical Symposium on Soil-Structure Interaction, Auckland, New Zealand, 2008.
5.  M. Cubrinovski, B. Bradley, Evaluation of seismic performance of geotechnical structures, International Conference on Performance-Based Design in Earthquake Geotechnical Engineering, Tsukuba, Japan, 2009.
6.  A. Zafeirakos, N. Gerolymos, V. Drosos, Incremental dynamic analysis of caisson-pier interaction, Soil Dynamics and Earthquake Engineering, 48 (2013) 71-88.
7.  B. Bradley, M. Cubrinovski, R. Dhakal, Performance-based seismic response of pile foundations, Geotechnical Earthquake Engineering and Soil Dynamics IV, ASCE Geotechnical Special Publication 181, Sacramento, USA, 2008.
8.  F. Chen, H. Takemiya, J. Shimabuku, Seismic Performance of a Wib-Enhanced Pile Foundation, The 13th World Conference on Earthquake Engineering, Paper No. 1273, Vancouver, Canada, 2004.
9.  B. Folic, R. Folic, Design methods analysis of seismic interactions soil-foundation-bridge structures for different foundations, NATO Advanced Research Workshop 983188: Coupled Site and Soil-Structure Interaction Effects with Application to Seismic Risk Mitigation, Borovets, Bulgaria, 2008.
10. W. Finn, Characterizing pile foundations for evaluation of performance based seismic design of critical lifeline structures, The 13th World Conference on Earthquake Engineering, Paper No. 5002, Vancouver, Canada, 2004.
11. H. Ghalibafian, C. Ventura, R. Foschi, Effects of nonlinear soil-structure interaction on the inelastic seismic demand of pile-supported bridge piers, The 14th World Conference on Earthquake Engineering, Beijing, China, 2008.
12. M. Alfach, Influence of soil plasticity on the seismic performance of pile foundations - a 3D numerical analysis, Jordan Journal of Civil Engineering, 6(4) (2012) 394-409.
13. T. Maki, S. Tsuchiya, T. Watanabe, K. Maekawa, seismic response analysis of pile foundation using finite element method, The 14th World Conference on Earthquake Engineering, Beijing, China, 2008.
14. T. Thavaraj, W. Finn, G. Wu, Seismic response analysis of pile foundations, Geotechnical and Geological Engineering, 28(3) (2010) 275-286.
15. M. Teguh, C. Duffield, A. Mendis, G. Hutchinson, Seismic performance of pile-to-pile cap connections: an investigation of design issues, Electronic Journal of Structural Engineering (EJSE), 6(1) (2006) 8-18.
16. SeismoStruct: User Manual, 254p, 2012, URL: http://www.seismosoft.com
17. SeismoStruct, URL: http://www.seismosoft.com
18. J. Mander, M. Priestley, R. Park, Theoretical stress-strain model for confined concrete, Journal of Structural Engineering, 114(8) (1988) 1804-1825.
19. Eurocode 2, Design of Concrete Structures - Part 1-1: General Rules and Rules for Buildings, European Committee for Standardization, Brussels, Belgium, 2003.
20. J. Simo, T. Hughes, Computational Inelasticity, Springer-Verlag, New York, USA, 1998.

21. J. Hellesland, A. Scordelis, Analysis of RC bridge columns under imposed deformations, IABSE Colloquium, Delft, Holland, 1981, pp. 545-559.
22. C. Fellipa, Nonlinear Finite Element Methods, University of Colorado, Boulder, USA, 2007.
23. N. Allotey, M. El Naggar, A numerical study into lateral cyclic nonlinear soil-pile response, Canadian Geotechnical Journal, 45(9) (2008) 1268-1281.
24. N. Allotey, El M. Naggar, Generalized dynamic winkler model for nonlinear soil-structure interaction analysis, Canadian Geotechnical Journal, 45(4) (2008) 560-573.
25. M. Ćosić, S. Brčić, Ground motion processing methodology for linear and nonlinear seismic analysis of structures, Journal of Construction (seriban), 66(11-12) (2012) 511-526.
26. Y. Fahjan, Selection, scaling and simulation of input ground motion for time history analysis of structures, Seminar on Earthquake Engineering and Historic Masonry, University of Minho, Braga, Portugal, 2010.
27. D. Gasparini, E. Vanmarcke, Simulated Earthquake Motions Compatible with Prescribed Response Spectra, Massachusetts Institute of Technology, Boston, USA, 1976.
28. S. Kramer, Geotechnical Earthquake Engineering, Prentice Hall, Upper Saddle River, USA, 1996.
29. D. Vamvatsikos, A. Cornell, Applied incremental dynamic analysis, Earthquake Spectra, 20(2) (2004) 523-553.
30. M. Ćosić, About the required number and size of increments in incremental nonlinear dynamic analysis, GNP 2010, Civil Engineering - Science and Practice, Žabljak, Montenegro, 2010.
31. H. Hilber, T. Hughes, R. Taylor, Improved numerical dissipation for time integration algorithms in structural dynamics, Earthquake Engineering and Structural Dynamics, 5(3) (1977) 283-292.
32. Simqke: URL: http://dicata.ing.unibs.it/gelfi/software/simqke/simqke_gr.htm
33. Eurocode 8, Design of Structures for Earthquake Resistance - Part 1: General Rules, Seismic Actions and Rules for Buildings, European Committee for Standardization, Brussels, Belgium, 2004.
34. Shake: URL: http://www.proshake.com
35. SEAOC Blue book: Recommended Lateral Force Requirements and Commentary, Report prepared by Structural Engineers Association of California, Sacramento, USA, 1999.
36. FEMA 356, Pre-Standard and Commentary for the Seismic Rehabilitation of Buildings, American Society of Civil Engineers, Federal Emergency Management Agency, Washington D.C., USA, 2000.
37. HAZUS, Earthquake Loss Estimation Methodology, National Institute of Building for the Federal Emergency Management Agency, Washington D.C., USA, 1997.
38. E. Choi, R. DesRoches, B. Nielson, Seismic fragility of typical bridges in moderate seismic zones, Engineering Structures, 26(2) (2004) 187-199.
39. N. Johnson, K. Samuel, N. Balakrishnan, Continuous Univariate Distributions, Vol. 1, Wiley-Interscience, New York, USA, 1994.
40. F. Nateghi-a, V. Shahsavar, Development of fragility and reliability curves for seismic evaluations of a major prestressed concrete bridge, The 13th World Conference on Earthquake Engineering, Paper No. 1351, Vancouver, Canada, 2004.

# ANALIZA POVREDLJIVOSTI I POUZDANOSTI INTERAKCIJE TLO - ŠIP - STUB MOST

U radu je prikazana procedura evaluacije seizmičkih performansi interakcije šip-tlo inkrementalnom nelinearnom dinamičkom analizom (INDA - Incremental Nonlinear Dynamic Analysis). Ulazni signal u sistemu je tretiran preko generisanih veštačkih akcelerograma, a koji su dodatno procesirani po slojevima tla do osnovne stene. Postprocesiranje INDA analiza izvršeno je posebno za stub, a posebno za šip, tako da su konstruisane krive PGA=f(DR) u kapacitativnom domenu. Za ovako konstruisane krive određeni su performansni nivoi, a na osnovu određenih DR i PGA parametara sprovedene su regresione analize. Krive povredljivosti su konstruisane na osnovu rešenja regresione analize i teorije verovatnoće log-normalne raspodele. Takođe, konstruisane su i krive pouzdanosti na osnovu rešenja analize povredljivosti. Metodološki postupak za analizu seizmičkih performansi, prezentovan u ovom istraživanju, omogućava integrisano kvantitativno-kvalitativno razmatranje i evaluaciju kompleksne interakcije konstrukcija-tlo (SFSI - Soil-Foundation-Structure Interaction).

Ključne reči: inkrementalna nelinearna dinamička analiza, performanse šipova, povredljivost, pouzdanost, veštački akcelerogrami.